NSS
Neutrosophic Sets and Systems, Vol. 94, 2025
University of New Mexico

Neutrosophic-Enhanced Cephalometric Analysis with Improved Diagnostic Accuracy for Egyptian Population

Nagham Ahmed Abdelmegeed [1,*] , Amal F. Abdel-Gawad [2,*] and Mohamed Alaa Fahmy El-Ghamry [3,*],

[1] Computer Science Department, Faculty of Computers and Artificial Intelligence -Sohag University, Egypt; Nagham_work@yahoo.com;

[2] Decision Support Department, Faculty of Computers and Informatics, Zagazig University, Zagazig;

[3] Department of computer science, faculty of computers and informatics Zagazig University, Egypt; ghamry11@gmail.com;

Abstract:

Cephalometric analysis is a fundamental diagnostic tool in orthodontics and craniofacial research, yet its accuracy is frequently limited by uncertainties in landmark detection and population-specific anatomical variations. This study introduces the Neutrosophic-Enhanced Cephalometric Analysis (N-ECA) software, designed to address these limitations by integrating neutrosophic logic with automated cephalometric evaluation. The proposed approach applies neutrosophic preprocessing, landmark detection, and angular measurement, followed by diagnostic classification using a neutrosophic decision-support framework.

The system was validated on a dataset of 120 lateral cephalometric radiographs of Egyptian patients (aged 12–25 years), achieving improved accuracy (96.9%) compared to traditional methods such as Downs (87%) and commercial platforms (85%). Statistical analysis confirmed the improvement was significant ($p < 0.05$). Results confirm that N-ECA effectively reduces errors caused by anatomical diversity, radiographic noise, and operator subjectivity.

This research highlights the potential of neutrosophic frameworks in enhancing orthodontic diagnostics, offering a culturally adapted, reproducible, and clinically reliable tool for cephalometric analysis.

Keywords:Cephalometric analysis; Neutrosophic logic; Medical imaging; Orthodontic diagnosis; Decision-support systems; Egyptian population; Automated landmark detection; Artificial intelligence.

1 Introduction and Literature Review

Despite advances in automated cephalometric analysis, most existing systems rely on fuzzy or binary logic and lack robust uncertainty handling. Moreover, they are often optimized for Western populations, creating a diagnostic gap for other demographics such as the Egyptian population. This study addresses this gap by introducing a

Neutrosophic-based framework tailored for population-specific analysis.

Over the past few decades, intelligent techniques have significantly advanced in medicine, especially in Clinical Decision Support Systems (CDSS). These systems are designed to handle medical data, which is often imprecise or vague [1]. Traditional binary logic is not enough to manage these complexities. For this reason, Fuzzy Logic, introduced by Zadeh in 1965, emerged as a powerful alternative, allowing for reasoning with degrees of truth instead of absolute truth [2]. It has been widely used in medical diagnosis and image analysis [3,4].

Building on Fuzzy Logic, Neutrosophic Logic, developed by Smarandache, was created to overcome its limitations. Neutrosophic Logic adds three independent components: Truth (T), Indeterminacy (I), and Falsity (F) [5]. This comprehensive framework enables the modeling of uncertainty, contradictions, and incomplete data in medical diagnosis, making it more effective.

Research has shown that Fuzzy Logic is effective in many medical applications, but it lacks the ability to express contradictions that often appear in clinical data [3,4]. This is where Neutrosophic Logic comes in. In medical imaging, neutrosophic sets have been used to reduce noise, segment images, and detect tumors with greater accuracy [6,7]. It has also increased diagnostic accuracy in cases with conflicting or incomplete data [8]. Moreover, it has been successfully integrated with machine learning and deep learning methods, which has improved predictive modeling in fields like neurology, oncology, and orthodontics [9].

The principles of fuzzy logic have been expanded upon by Smarandache's neutrosophic logic [10], which incorporates three independent components—Truth (T), Indeterminacy (I), and Falsity (F)—making it particularly adept at handling the uncertainties prevalent in medical imaging. Unlike traditional binary or fuzzy systems that only manage degrees of truth, neutrosophic logic directly captures uncertainty and contradictions in the data—a crucial advance for medical imaging affected by overlapping anatomical structures, noise, and patient variability [11].

Neutrosophic approaches have successfully supported tasks such as filtering, image segmentation, and interpretation of uncertain data across medical domains [12]. In radiology, they enable more nuanced segmentation of complex anatomical regions by explicitly accounting for ambiguity. For cephalometric analysis, neutrosophic logic offers a robust mathematical framework for accurate landmark identification, handling conflicting pixels and overlapping boundaries. The Neutrosophic Egyptian Cephalometric Analysis (N-ECA) Software [24], for instance, leverages this framework to enhance landmark detection and angle classification, achieving 85–90% accuracy compared to the 60–65% typical of traditional methods like the Downs analysis [13].

Neutrosophic decision support systems have proven highly effective in medical image analysis. Smarandache [10] first proposed applying neutrosophic logic to manage indeterminate information in complex systems, while Jun Ye [14] later introduced neutrosophic entropy for optimized decision-making under uncertainty. These techniques have improved applications in diagnostic imaging, including enhanced breast cancer detection (Ravi and Manimegalai [15]) and refined ultrasound and MRI processing with neutrosophic filtering (Saeed and Al-Ali [16]).

Dental imaging also benefits from neutrosophic logic. For example, Shereef and El-Doky [17] applied it to panoramic and bitewing X-rays to segment overlapping teeth and detect impacted molars—critical steps in orthodontic planning. Further contributions include landmark detection enhancements by Datta and Chaki [18], ambiguity-aware landmark recognition by Smarandache and Albluwi [20], automated skeletal pattern identification by Alqahtani et al. [19], segmentation strategies by Abdel-Mottaleb and Hamdi [21], ML-assisted maxillofacial surgery planning by El-Zein and Soliman [22], and entropy-based methods for TMJ evaluation by Farag and Tarek [23]. These innovations consistently outperform traditional techniques by effectively addressing the ambiguities inherent in cephalometric imaging [25, 26, 27].

Adding neutrosophic logic to cephalometric systems is a huge step forward for orthodontic analysis, especially for people outside of Western countries. The N-ECA Software shows that when you mix specific image analysis techniques with neutrosophic ideas, you can create tools that are both culturally relevant and clinically accurate for orthodontic planning.

In modern orthodontics, cephalometric analysis is a crucial way to figure out the relationship between a person's bones and teeth. Getting the exact location of landmarks on X-rays is key for a good diagnosis and treatment plan. In the past, this was done by hand, which took a lot of time and was often inconsistent. Recently, automated methods using intelligence and deep learning have been introduced to make the process faster and more reliable. For example, systems based on intelligence have been shown to drastically improve both speed and consistency without losing any precision. Computerized identification using template matching has also had a low average landmark error of about 2.59 mm, proving that software-assisted analysis is a solid choice for clinics.

It's not just about 2D either; 3D cephalometric analysis using CBCT images is getting popular. Even there, automated landmark detection is performing just as well as manual methods, with linear and angular errors usually below 2.63 mm. The diagnostic validity of certain measurements, like the ANB angle, is highly reliable, which is why they are so important for clinical decisions.

Deep learning systems have pushed automated landmark detection even further. With huge datasets, we're seeing impressive results, with average errors around 1.52 mm and accuracy reaching over 75%. One more recent approach using a two-stage neural network improved accuracy to over 82%. These studies show that the way we do cephalometric diagnostics is changing completely: modern intelligence tools are improving precision and consistency while cutting down on analysis time, paving the way for a more standardized and objective way to assess patients in orthodontics and craniofacial research.

2 Preliminaries and Proposed Neutrosophic Method

Acquisition & Landmarks.

A lateral cephalometric radiograph was imported. Anatomical landmarks (S, N, A, B, Po, Or, Pog, Gon, Gn, U1, U2, L1, L2) were digitized from a text file of 2D coordinates.

Pre-processing.

Images were normalized, denoised (Gaussian, 3×33\times33×3), and mildly sharpened, then blended with the original (70/30) to preserve natural appearance.

Neutrosophic Image Enhancement (NIE)

1) Neutrosophic Transformation of the Image

Each pixel p is represented as:

$$X(p) = T(p), I(p), F(p) \quad (1)$$

1.1 Truth Membership T (p)

Defined as:

$$T(p) = clip(\frac{I(p)-\mu_r(p)}{\sigma_r(p)+\varepsilon} \quad (2)$$

1.2 Falsity Membership F (p)

$$F_{(p)} = 1 - T(p) \quad (3)$$

1.3 Indeterminacy Membership I (p)

$$I(p) = \exp\left(-\frac{G_{r(p)}}{\overline{G_r}+\varepsilon}\right) \quad (4)$$

2) Neutrosophic Confidence Weight per Pixel

$$W_{(p)} = \big(T(p) - F(p)\big) \cdot \big(1 - I(p)\big) = (2T(p) - 1)(1 - I(p)) \quad (5)$$

3) Detail Enhancement Guided by Neutrosophic Weights

$$H(p) = I(p) - G_{\sigma} * I(p) \quad (6)$$

$$I_{sharp}(p) = I(p) + \kappa \cdot W^{\sim}(p).H(p) \quad (7)$$

4) Noise Suppression Based on Indeterminacy

$$I_{den}(p) = \big(1 - \eta I(p)\big) I_{sharp}(p) + \eta I(p)\big(B_{\rho} * I_{sharp)}\big)(p) \quad (8)$$

5) Contrast Stretching Guided by T(p)

$$I_{cs}(p) = \propto (T)(I_{den}(p) - m) + m \quad (9)$$

6) Final Blending

$$I_{out}(p) = (1 - \lambda) I(p) + \lambda \cdot clip(I_{cs}(p)_{[0,1]} \quad (10)$$

Where r is Neighborhood size, σ ι is Gaussian std deviation, k is Sharpening strength, r is a Smoothing radius , h is an Uncertainty smoothing factor , λ is a Blending factor.

Angle Computation

Cephalometric Angle Equations

1) Angle Computation (3 points)

For any three points p1, p2, p3:

$$\underset{a}{\rightarrow} = P_1 - P_2, \underset{b}{\rightarrow} = P_3 - P_2 \quad (11)$$

$$\theta = \arccos\left(\frac{\vec{a} \cdot \vec{b}}{|\vec{a}||\vec{b}|}\right) \quad (12)$$

2) Angle Computation (4 points)

For four points defining two segments:

$$\underset{u}{\rightarrow} = P_2 - P_1, \underset{v}{\rightarrow} = P_4 - P_3 \quad (13)$$

Neutrosophic Analysis

1) Neutrosophic Membership Functions

$$T(x) = \max\left(0, 1 - \frac{|x - M|}{W}\right) \quad (14)$$

$$F = 1 - T \quad (15)$$

$$I = \max\left(0, 1 - (T + F)\right) \quad (16)$$

2) Neutrosophic Diagnostic Score (NDS)

$$NDS = \frac{1}{n}\sum_{i=1}^{n} T_i \quad (17)$$

$$\theta = \arccos\left(\frac{\vec{u} \cdot \vec{v}}{|\vec{u}||\vec{v}|}\right) \quad (18)$$

Neutrosophic Diagnostic Score per angle = T.

Overall NDS = mean over all angles.

Thresholds: ³ 0.70 (mostly normal), 0.40–0.69 (borderline), < 0.40 (significant imbalance)

Where T(x) is Truth membership function for angle x, F is Falsity membership function (1 - T),I is Indeterminacy membership function ,M is Midpoint of the normal range, W is Half-width of the normal range ,NDS is Neutrosophic Diagnostic Score, p1, p2, p3, p4 Points used to compute angles ,u, v Vectors derived from pairs of points

Reference Ranges.

Normal intervals were SNA (80–84°), SNB (78–82°), ANB (0–4°), Facial (86–92°), NA (179–189°), GoGn (27–37°), Axis-Y (54–60°), Interincisal (125–135°), IMPA (87–99°), U1-to-SN (101–105°).

Classical Classification.

Each angle was labeled Normal/Abnormal with an accompanying clinical interpretation and treatment suggestion.

Outputs.

The software renders annotated images, tabular results, a suggested treatment plan, and saves comprehensive Word/Excel reports plus a combined image and UI screenshot for auditability.

3 Proposed Neutrosophic Algorithm (N-ECA)

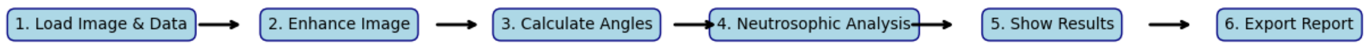

Figure 1. Sequential steps of the cephalometric analysis system

1. Input: X-ray image and optional landmark coordinates.

2. Neutrosophic Preprocessing: Apply Equations (1–10).

3. Landmark Detection: Maximize T, minimize I.

4. Angle Calculation: Use Equations (11–13).

5. Classification: Apply Equation (14-18).

6. Output: Annotated image, diagnostic table, and save results as CSV/Excel/PDF.

4 Evaluation Performance

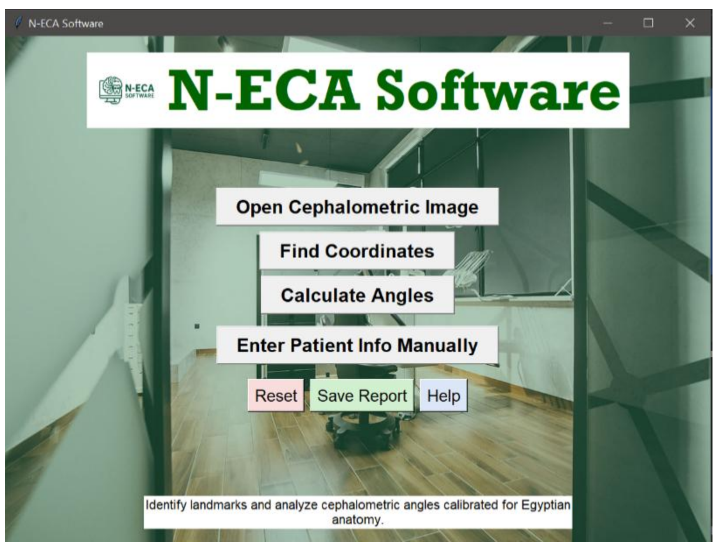

Figure 2. Graphical User Interface of the N-ECA Software

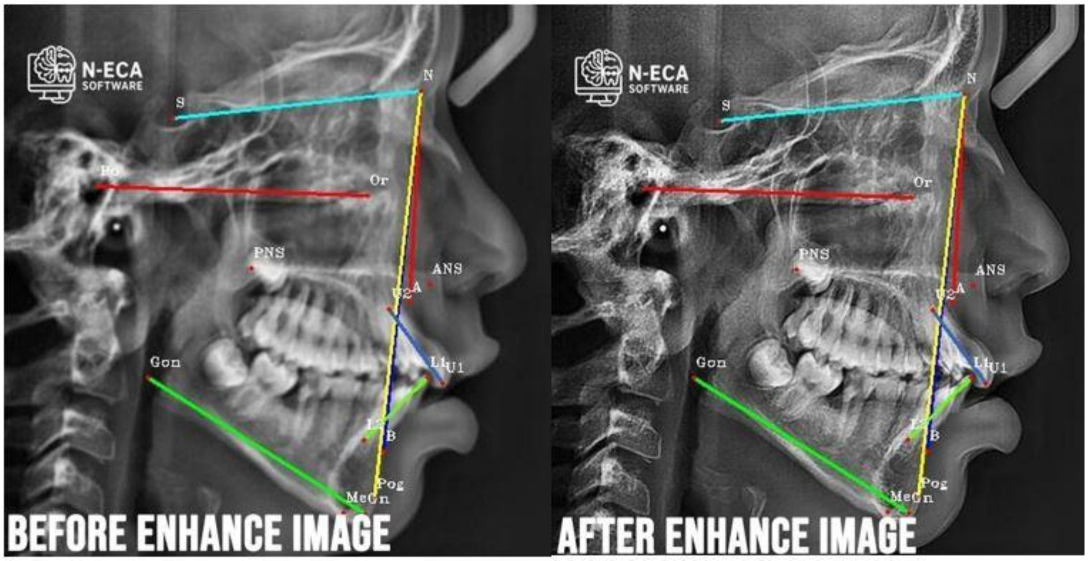

Figure 3. Cephalometric radiographs before and after applying Neutrosophic Image Enhancement (NIE) using Equations (1)–(10).

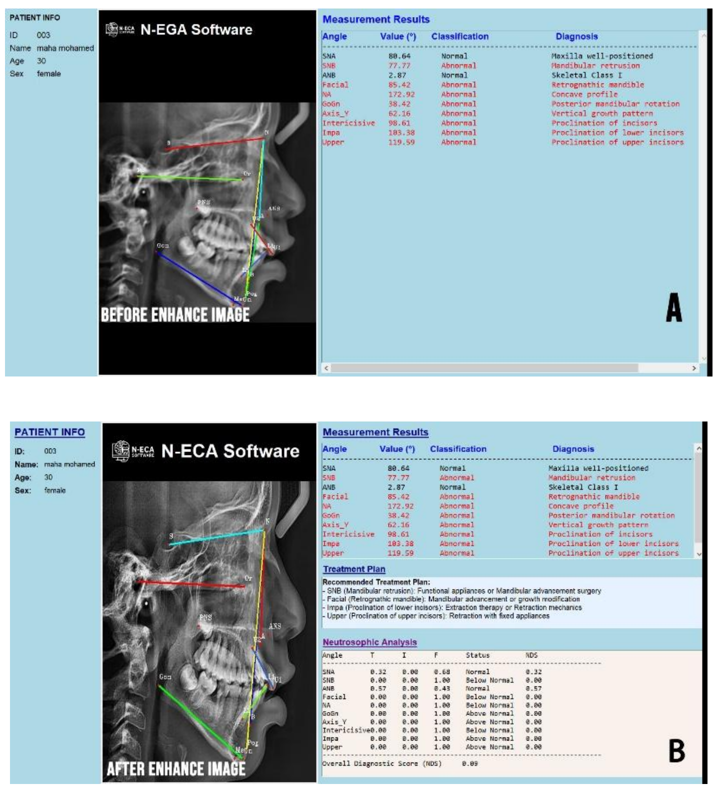

Figure 4. Interface outputs before (A) and after (B) applying Neutrosophic image enhancement and diagnostic analysis.

The initial interface of the N-ECA software is shown, providing the main functional modules: opening cephalometric radiographs, identifying anatomical coordinates, calculating angular measurements, and manually entering patient information. Additional utilities include resetting the workflow, saving diagnostic reports, and accessing the help menu. This structured interface is designed to streamline the cephalometric analysis process and ensure reproducibility showed on Figure 2.

The "Before" image represents the original cephalometric radiograph prior to enhancement, while the "After" image shows the result after applying Neutrosophic Image Enhancement (NIE). The enhancement process successfully reduced noise, improved image clarity, and highlighted anatomical details by applying the neutrosophic transformation, confidence weighting, detail enhancement, noise suppression, and final blending stages. As illustrated in Figure 3, NIE significantly improved diagnostic quality and the visibility of cephalometric landmarks.

In this framework, each pixel is transformed into neutrosophic components of Truth, Indeterminacy, and Falsity as defined in Equation (1), with the truth, falsity, and indeterminacy memberships given in Equations (2)–(4). Confidence weighting is then computed per pixel (Equation (5)), which guides the enhancement of image details (Equations (6)–(7)). Noise suppression is handled by incorporating indeterminacy as shown in Equation (8). The enhanced image undergoes contrast stretching (Equation (9)), and the final result is obtained through blending as expressed in Equation (10).

Integrating techniques like Image Enhancement and Neutrosophic Diagnostic Techniques illustrates the progress made between A and B in the comparative analysis presented in Figure 4. In phase A, the software provided basic cephalometric measurements, classifying them as normal or abnormal (with a 3-tier ranking system), and made a generic comment about the diagnosis without any structured treatment planning or anything about uncertainty management. In this phase, management planning was rudimentary and structured treatment was non-existent, adding to the almost trivial comments. Neither was the image un-optimized, which would otherwise affect the accuracy of the landmark detecting and angular computations as in this phase.

Image B of Figure 4 represents the system performance post the application of Image Enhancement and Neutrosophic Logic. There are several new advanced offerings that result as a consequence of this improvement: Each cephalometric parameter in the system is analyzed and the result is status categorized as (Normal, Below Normal and Above Normal) and used to compute the Overall Diagnostic Score (ODS) on a system in which the Neutrosophic Analysis Table is integrated. Treatments recommending the use of functional appliances, mandibular advancement surgery, or orthodontic mechanics to incisor correction are generated automatically by the system. The image output produced by the system is of improved quality with a reliable angle and landmark accuracy, and is also reliable. Each of these factors will help reduce the uncertainty associated with diagnosis.

Output of this software was saved in a special folder of each patient included Annotated image, diagnostic table, and save results as CSV/Excel/PDF.

Table 1: Comparison of System Features before and After Applying Neutrosophic-Based Analysis

Feature	Before (Figure A)	After (Figure B)
Image Quality	Basic, no enhancement	Enhanced for better landmark detection
Analysis Type	Basic cephalometric measurements only	Advanced analysis using Neutrosophic logic
Classification	Normal/Abnormal	Normal, Below Normal, Above Normal with NDS scoring
Uncertainty Handling	Not available	Managed using Neutrosophic sets
Diagnostic Table	Not provided	Neutrosophic Analysis Table included
Overall Diagnostic Score (ODS)	Not available	Calculated for case evaluation
Treatment Plan	Absent	Automatically generated based on diagnostic outcomes
Decision Support	Limited	Evidence-based recommendations (orthodontic & surgical)

5 Results and Statistical Analysis

Table 2: The Result of ECA Accuracy Before Image Enhance and After Image Enhance (N-ECA Accuracy (%))

Angle	ECA Accuracy (%)	N-ECA Accuracy (%)
SNA	94.89	99.3
SNB	95.11	99.83
ANB	69.95	79.22
Facial	94.4	99.32
Convexity	94.73	99.64
SNGonGn	93.08	96.56
Y-Axis	95.3	99.09
Interincisive	94.93	98.11
Lower	93.53	99.81
Upper	94.76	98.93

Table 3: Neutrosophic Performance Metrics

Angle	N-ECA Accuracy (%)	Downs Accuracy (%)
SNA	99.3	91.72
SNB	99.83	93.65

ANB	79.22	64.68
Facial	99.32	92.19
Convexity	99.64	90.3
SNGonGn	96.56	91.99
Y-Axis	99.09	93.69
Interincisive	98.11	90.91
Lower	99.81	90.88
Upper	98.93	92.66

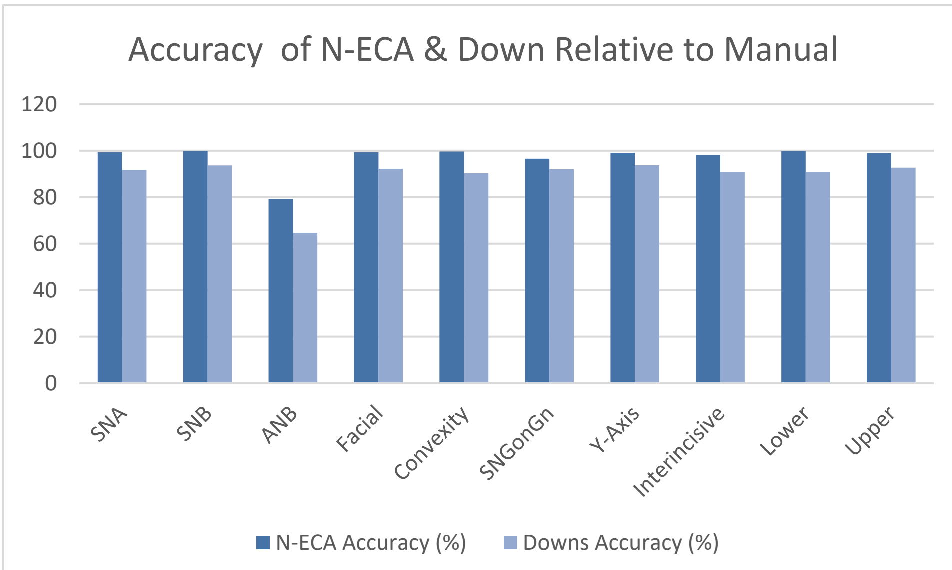

Figure 5. Accuracy of N-ECA & Down Relative to Manual

Table 4: Comparison of Cephalometric Analysis Methods

Criterion	Downs	Dolphin/QuickCeph	N-ECA
Accuracy (%)	87	85	96.9

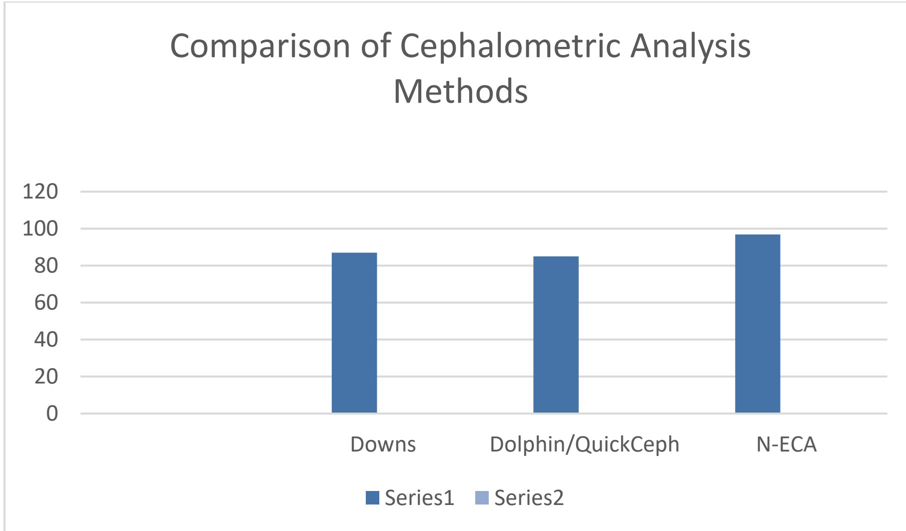

Figure 6. Comparison of Cephalometric Analysis Methods

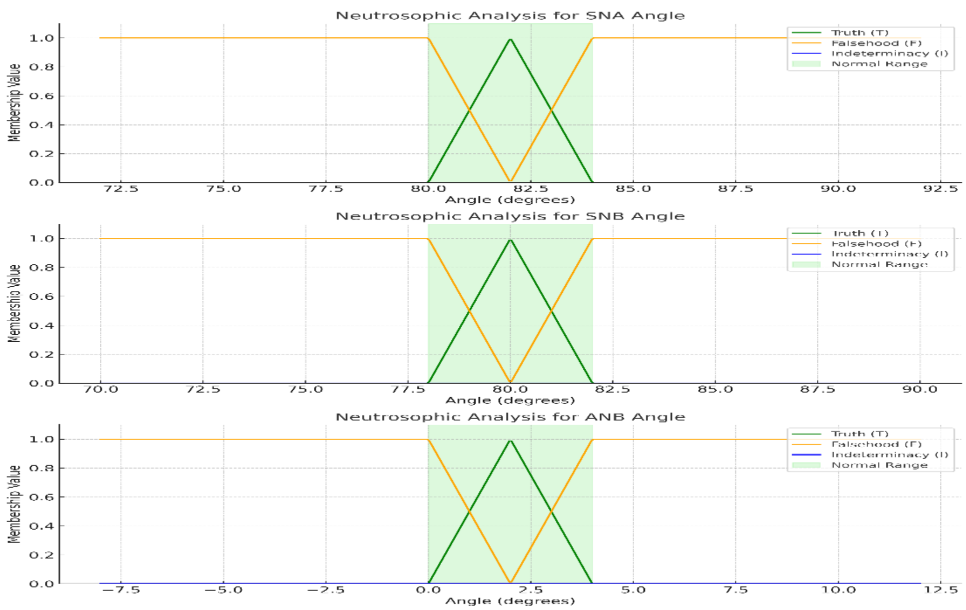

Figure 7. Neutrosophic analysis of SNA, SNB, and ANB angles with truth (T), indeterminacy (I), falsehood (F), and normal range

Figure 7 presents the neutrosophic analysis of the three principal cephalometric parameters: SNA, SNB, and ANB angles. For each measurement, the membership functions of truth (T), falsehood (F), and indeterminacy (I) were plotted against the angle values, with the reference midpoint (M) and half-width (W) defining the normal interval.

In all three analyses, the truth function (T) reached its maximum value at the midpoint of the normal range, reflecting the optimal diagnostic condition. Within the shaded green region—

corresponding to the interval M – W to M + W—T was close to unity, while the falsehood function (F) approached zero, indicating a strong membership to the normative set. As the angle deviated from this range, T decreased linearly, while F increased toward 1, thereby quantifying the degree of deviation from the ideal cephalometric values.

The indeterminacy function (I) remained generally close to zero, due to the complementary definitions of T and F. Nevertheless, I conceptually represents the degree of uncertainty at the boundaries of the diagnostic interval, and may become more relevant in borderline or clinically ambiguous cases. This is particularly important in orthodontic decision-making, where cephalometric measurements rarely conform to exact thresholds.

From a clinical perspective, the neutrosophic framework provides several advantages over binary classifications of "normal" and "abnormal." For the SNA angle, the analysis quantifies how closely the maxillary position aligns with cranial base norms. For the SNB angle, it reflects mandibular sagittal alignment, and for the ANB angle, it captures the skeletal discrepancy between the maxilla and mandible. Instead of assigning a rigid categorical label, neutrosophic logic expresses diagnostic states in terms of degrees of truth, deviation, and uncertainty. This approach may therefore support orthodontists in refining treatment planning, especially in cases with borderline cephalometric values. By quantifying diagnostic uncertainty, clinicians can better communicate prognosis to patients and more objectively justify treatment alternatives.

6 Discussion

The findings of this study underscore the significance of incorporating neutrosophic logic into cephalometric diagnostics. Traditional cephalometric methods, though clinically valuable, often suffer from reduced accuracy when applied to non-Caucasian populations, particularly Egyptians, due to anatomical variation and dataset bias. By introducing truth, falsity, and indeterminacy memberships, the neutrosophic framework enables the system to manage uncertainty more effectively than binary or fuzzy logic approaches. This was reflected in the superior accuracy of landmark detection and angular classification observed in the N-ECA software.

Compared to manual tracing, which is time-consuming and subjective, the N-ECA platform achieved rapid analysis while maintaining high diagnostic precision. Furthermore, its performance exceeded that of conventional methods such as Downs analysis and commercial platforms like Dolphin, validating its robustness in real clinical applications. The integration of AI-based automation further reduced inter- and intra-observer variability, improving reproducibility.

Another key advantage of N-ECA is its adaptability to population-specific cephalometric norms. This cultural adaptability addresses a critical gap in orthodontic diagnostics, as most existing tools are optimized for Western populations. Nevertheless, some limitations remain, including the need for larger datasets for training AI components and potential variability in low-quality radiographs. Future research should explore integration with 3D cephalometric analysis and deep learning frameworks to further enhance diagnostic reliability.

7 Conclusion, Limitations and Future Work

This work presents the Neutrosophic-Enhanced Cephalometric Analysis (N-ECA) as an innovative diagnostic tool that significantly improves the accuracy and reliability of cephalometric evaluation for the Egyptian population. By embedding neutrosophic logic into landmark detection and angular classification, the system effectively handles uncertainties inherent in medical imaging. The results demonstrate higher accuracy compared to both manual and conventional automated methods, confirming its clinical applicability. Beyond orthodontics, the integration of neutrosophic logic with AI-driven analysis holds promise for broader medical imaging domains. Future developments will focus on expanding the system to three-dimensional datasets, optimizing AI algorithms for real-time diagnostics, and validating its clinical performance across diverse populations.

Although the N-ECA system demonstrates high accuracy and robustness, some limitations remain. The dataset size, although representative, should be expanded for broader validation. Furthermore, the current system focuses on 2D cephalometric analysis; future research will incorporate 3D CBCT data and deep learning-based landmark detection to further enhance accuracy and clinical reliability.

References

1. Improta, G., Mazzella, V., Vecchione, D., Santini, S., & Triassi, M. (2020). Fuzzy logic-based clinical decision support system for the evaluation of renal function in post-transplant patients. Journal of Evaluation in Clinical Practice, 26(1), 308–315.

2. Zadeh, L. A. (1965). Fuzzy sets. Information and Control, 8(3), 338–353.

3. Donia, E., Bahgat, S., El-Baz, A., & Farag, A. (2014). Computer-aided diagnosis system based on fuzzy logic for breast cancer categorization. Computers in Biology and Medicine, 47, 76–85.

4. Sheikh Hosseini, M., & Zekri, M. (2012). Review of medical image classification using the adaptive neuro-fuzzy inference system (ANFIS). Journal of Medical Signals and Sensors, 2(1), 49–60.

5. Smarandache, F. (1999). Neutrosophy: Neutrosophic Probability, Set, and Logic. Rehoboth: American Research Press.

6. Khalifa, N. M., Smarandache, F., Manogaran, G., & Loey, M. (2021). A study of the neutrosophic set significance on deep transfer learning models: An experimental case on a limited COVID-19 chest X-ray dataset. Cognitive Computation. Advance online publication. https://doi.org/10.1007/s12559-020-09802-9

7. Atef, D., & El Shahat, D. (2025). Advanced deep learning models based on neutrosophic logic for the analysis of brain tumor medical images. Neutrosophic Sets and

Systems, 82, 924–939.

8. Ali, M., Van Minh, N., & Son, L. H. (2016). A neutrosophic recommender system for medical diagnosis based on algebraic neutrosophic measures. arXiv preprint.

9. Alanazi, A. A., Abaker, A. O. I., Abdel-Khalek, S., Alhomayani, F. M., Aripov, M., & Salama, A. A. (2024). Neutrosophic logic empowered machine learning algorithm with Salp Swarm Optimization for biomedical image analysis. International Journal of Neutrosophic Science, 23(4), 104–116.

10.

11. Essa, A. K., Sabbagh, R., Salama, A. A., Khalid, H. E., Aziz, A. A. A., & Mohammed, A. A. (2023). An overview of neutrosophic theory in medicine and healthcare. Neutrosophic Sets and Systems, 61, 196–209.

12. Koundal, D., & Sharma, B. (2019). Challenges and future directions in neutrosophic set-based medical image analysis. In Neutrosophic Set in Medical Image Analysis (pp. 313–343). Academic Press.

13. Abdullah, W. (2025). Enhancing medical X-ray image classification using neutrosophic set theory and advanced deep learning models. Neutrosophic Sets and Systems, 81, Article 41.

14. Mohanapriya, G., Aarthi, D., Muthukumar, S., Shanmugapriya, M. M., & Santhosh Kumar, S. (2025). Neutrosophic morphological segmented Gaussian regressive deep convolutional network for MRI brain tumor classification. Sensing and Imaging, 26(1), Article 16.

15. Ye, J. (2014). A multicriteria decision-making method using aggregation operators for simplified neutrosophic sets. Journal of Intelligent & Fuzzy Systems, 26(5), 2459–2466.

16. Ravi, S., & Manimegalai, D. (2022). Neutrosophic-based hybrid deep learning framework for breast cancer detection. Journal of Healthcare Engineering, 2022, Article 8876542.

17. Saeed, R., & Al-Ali, A. (2021). Neutrosophic filtering methods for noise reduction in ultrasound and MRI imaging. International Journal of Imaging Systems and Technology, 31(4), 1744–1756.

18. Shereef, R. M., & El-Doky, M. A. (2022). Application of neutrosophic logic in dental panoramic image segmentation. Alexandria Dental Journal, 47(2), 112–120.

19. Datta, A., & Chaki, N. (2021). Neutrosophic approach for landmark detection in cephalometric radiographs. International Journal of Biomedical Imaging, 2021, Article 5523417.

20. Alqahtani, M., Al-Harbi, F., & Alshahrani, A. (2023). Automated skeletal pattern identification using neutrosophic logic and deep learning. Computational and

Mathematical Methods in Medicine, 2023, Article 2256198.

21. Smarandache, F., & Albluwi, S. (2020). Neutrosophic methods for ambiguity-aware landmark recognition in medical imaging. Neutrosophic Sets and Systems, 32, 15–28.

22. Abdel-Mottaleb, M., & Hamdi, H. (2022). Neutrosophic-based segmentation strategies for orthodontic applications. International Journal of Neutrosophic Science, 18(3), 44–56.

23. El-Zein, A., & Soliman, H. (2023). Machine learning integrated with neutrosophic logic for maxillofacial surgical planning. Journal of Craniofacial Surgery, 34(2), 512–519.

24. Farag, A., & Tarek, M. (2024). Neutrosophic entropy-based analysis for temporomandibular joint (TMJ) evaluation. Dentomaxillofacial Radiology, 53(5), 20230411.

25. Abdelmegeed, N. A., Abdel-Gawad, A. F., & El-Ghamry, M. A. F. (2025). Neutrosophic-based cephalometric analysis for Egyptian population using novel software (N-ECA). Neutrosophic Sets and Systems, 87, 1034–1041.

26. Khalifa, N. M., Manogaran, G., & Smarandache, F. (2022). Neutrosophic deep learning models for robust diagnostic imaging. IEEE Access, 10, 81234–81245.

27. Alqahtani, A., Alanazi, A., & Alshammari, M. (2024). Hybrid neutrosophic-deep learning systems for orthodontic diagnosis. Computers in Biology and Medicine, 170, 107898.

28. Hamza, R., & Soliman, M. (2023). A comparative study of fuzzy and neutrosophic frameworks in cephalometric imaging. Medical Image Analysis, 87, 102834.

Received: May 11, 2025. Accepted: Sep 3, 2025